STUDY ON NANOSTRUCTURED MOLYBDENUM CARBIDE FOR HYDROGEN EVOLUTION REACTION

by

Anqi Wang

B.S, Nanjing University, 2015

Submitted to the Graduate Faculty of

Swanson School of Engineering in partial fulfillment

of the requirements for the degree of

Master of Science

University of Pittsburgh

2017

UNIVERSITY OF PITTSBURGH

SWANSON SCHOOL OF ENGINEERING

This thesis was presented

by

Anqi Wang

It was defended on

March 27, 2017

and approved by

Jung-Kun Lee, PhD, Associate Professor

Department of Mechanical Engineering and Material Science

Ian Nettleship, PhD, Professor

Department of Mechanical Engineering and Material Science

Wissam Abdo Saidi, PhD, Professor

Department of Mechanical Engineering and Material Science

Thesis Advisor:

Jung-Kun Lee, PhD, Associate Professor

Department of Mechanical Engineering and Material Science

STUDY ON NANOSTRUCTURED MOLYBDENUM CARBIDE FOR HYDROGEN EVOLUTION REACTION

Anqi Wang, M.S.

University of Pittsburgh, 2017

Molybdenum carbide is one of candidates which can replace platinum for the application of hydrogen evolution reaction (HER). In previous studies, different synthesis methods were used to prepare multi-phases molybdenum carbide particles. However, these processes required high temperature annealing. In this thesis, the effect of microwave-assisted solvothermal (MWSV) reaction on the phase evolution of molybdenum carbide is studied. MWSV method is a combination of solvothermal reaction and microwave heating. The most advantage is vigorous agitation of molecules and internal heating, which can largely reduce reaction time. Highly crystalline Mo_2C is obtained by annealing resultants of MWSV at low temperature. A change in precursor compositions during MWSV has a significant impact on the crystal structure of final products. HER test shows that MWSV grown Mo_2C particles have an ability of proton reduction when low electric potential is applied.

TABLE OF CONTENTS

LIST OF TABLES

LIST OF FIGURES

NOMENCLATURE

HER Hydrogen evolution reaction

MWSV Microwave assisted solvothermal

TPR Temperature programmed reduction

FTO Fluorine doped tin oxide

LSV Liner sweep voltammetry

CV Cyclic voltammetry

SEM Scanning electron microscope

PEM Polymer electrolyte membrane

PGM Platinum-group metals

ACIWE Acid liquid electrolyte water electrolysis

ALKWE Alkaline liquid electrolyte water electrolysis

DFT Density functional theory

SCE Saturated calomel electrode

CNT Carbon nanotube

ACKNOWLEDGMENT

I would have great and sincere thanks to my advisor, Prof. Jung-Kun Lee for his patience, generousness and considerable help throughout my study and research. Without his guidance and support, I would have never accomplished my research.

I would also thank my committee members: Prof. Ian Nettleship, Prof. Wissam Abdo Saidi and Prof. Jung-Kun Lee for their time to make this thesis better.

I have my thanks to my excellent upper class students in my research group: Dr. Gill-Sang Han, Seongha Lee, Fangda Yu, Matthew Lawrence Duff for sharing priceless experience in experiments. My thanks also go to my lab partners: Salim Caliskan, Fen Qing for their kind help.

Finally, I would thank my family for their support and encouragement.

1.0 INTRODUCTION

Fast growth of high energy consumption technology and depletion of fossil energy resources have forced development of clean and renewable energy sources. Primary renewable energy sources, such as wind and tides, are environmental friendly. However, most of them suffer from daily and seasonal limitation and regional variability. To avoid these problems, these unstable energy sources can be translated into stable hydrogen energy by water electrolysis.[1] Since water is very stable chemical, water splitting is a challenging task. Some representative thermochemical water splitting technology such as hyperthermal hydrogen evolution and iodine-sulphur (IS) cycle way [2,3], have a limitation of high temperature requirement (above 1000℃), which prevent their extensive application.

Water splitting via photocatalytic and photo-electrochemical approaches has been a hot topic recently since it can directly use solar energy [4-6]. However, the low energy conversion efficiency limits large-scale production of hydrogen using solar energy. In comparison, water electrolysis shows excellent adaptability, which can efficiently produce hydrogen (or oxygen) from intermittent energy source via electrochemical energy devices. Instead of batteries, hydrogen is an alternative energy storage method and can be subsequently reconverted into electricity via fuel cells. [7]

Water electrolysis was first reported in 1789 [8], it has been widely studied since then. This method has high efficiency and flexibility, and can produce high-purity

hydrogen (≈100%). However, water electrolysis needs more affordable electrode and electrolyte material with long-term durability. Electrodes for the water electrolysis can be divided into a cathode causing hydrogen evolution reaction (HER) and an anode causing oxygen evolution reaction (OER). Depending on electrolyte materials, water electrolysis techniques are grouped into polymer electrolyte membrane (PEM) water electrolysis, acid liquid electrolyte water electrolysis (ACIWE) and alkaline liquid electrolyte water electrolysis (ALKWE). PEM water electrolysis is commonly used and available on the market. It can operate at high current densities (up to above 2 Acm^{-2}) and high pressures (over 150 bar), shown in Table 1 [9].

Table 1 Some parameter of polymer and liquid electrolyte electrolysis

Specifications	Polymer electrolyte electrolysis	Liquid electrolyte electrolysis
Electrolyzer Pressure (bar)	<150	<30
Current density(A cm^{-2})	0.6-2.0	0.2-0.4
Cell Voltage(V)	1.8-2.2	1.8-2.4
Power Density(W cm-2)	<4.4	<1
Voltage efficiency(%)	67-68	62-68
Cell area(m^2)	<0.03	<4
H_2 production rate($N.m^3h^{-1}$)	30	760
Lifetime(years)	10-20	20-30

But only a few electrode materials show high stability in this process. [10] But only a few electrode materials show high stability in this process. [10] Moreover, PEM electrolyte also showed worse long-term stability than liquid electrolyte devices. In the meantime, ALKWE is only able to operate at low current density and pressure, and also shows adequate chemical and mechanical stability. Recently, numerous non-precious catalysts have been found to have noble metal-like performance, and some of them even show better catalytic activity than traditional noble metal electrodes.[11]

Cathodic HER is a crucial half-cell reaction of electrochemical water splitting. Decomposition process of pure water into hydrogen can be described by the following equations:

$$\text{Cathode: } 2H^+(aq) + 2e^- \rightarrow H_2(g), E^o_{red} = 0.0V \quad (1.1)$$

The standard reduction potential for HER is 0V (vs. RHE) at 25℃, 1 atm. However, in an actual water electrolysis process, a larger applied potential is always required because it involves complex electron transfer processes, which leads to inactive kinetics and low energy efficiency. [12] During the water electrolysis, multiple disadvantageous factors of electrode materials should be considered such as solution and ion concentration, electrode resistance, electrolyte diffusion blockage, heat release and bubbles. [10] These factors make the actual potential higher than a theoretical value, which is called overpotential (η). Researchers have been working on improving electrolyzers and reducing energy loss. Here comes the nanostructured electrocatalysts, which could provide different transition states as more molecules

absorbed on the surface of electrodes to obtain enough energy to reach the transition state and meanwhile lower the activation energy. Thus, nanostructured electrocatalysts can increase the reaction rate or lower the potential requirement. Also, rational design of nanostructure and porous morphology will not only increase active reaction sites and reduce catalyst amount but also reduce the overpotential value. Among platinum-group metals (PGM), platinum is known as the most efficient HER electrocatalyst with almost zero overpotential and a low tafel slope which represents how much increase in the overpotential is required to increase the rate of HER. But also, all PGMs suffer from high cost and low reservation, which limit them for large-scale application. It is necessary to find more alternative materials with low cost and high efficiency to replace the PGMs electrodes in HER. Recently, some other metals like nickel and nickel-based alloys have been found to have high activity and long-term stability for ALKWE process. [10] In addition, some transition metal carbides, sulfide, phosphide and nitride have also developed as metal-free catalysts for the ACIWE process.

This thesis is organized in the following chapters. A brief introduction of hydrogen evolution reaction is introduced in chapter 1. Then followed with a review of HER mechanism and recent development of HER catalysts in chapter 2, also include the review of molybdenum carbide electrocatalyst and some previous methods of synthesizing nanostructured Mo_2C, analyze the advantages and disadvantages of those methods, and compare them with the newly microwave method which will be used in this thesis. Chapter 3 shows the hypothesis, objectives

and tasks of the experiment. Chapter 4 includes the experimental details from material synthesizing and electrodes making to measurements of materials and HER test for elctrocatalyst. Chapter 5 will show the results and data from the experiments, includes the SEM image of Mo_2C nanoparticles, J-V curves and Tafel plots of HER measurement. Chapter 6 is the overall conclusion and further works of this thesis.

2.0 BACKGROUND INFORMATION

2.1 FUNDAMENTALS OF HER

The HER mechanism is highly dependent on the pH value of electrolyte. As shown by the Nernst equation under standard condition (25℃, 1 atm), the Nernst potential referenced to normal hydrogen evolution(NHE) decreases linearly by 59mV per unit pH increase, and for RHE Nernst potential can be directly regarded as zero for any pH, the equation can be written as:

$$E_{RHE} = E^{0}_{(H_2/H^+)} - \frac{RT}{F} \times \ln(a_{H^+} / P_{H_2}^{1/2})$$
$$= -0.059 \times pH \text{Vvs.NHE} = 0\text{Vvs.RHE} \quad (2.1)$$

The Nernst potential shows the thermodynamic equilibrium potential that the reactions occur. However in real experimental section, the water electrolysis process needs a higher potential to overcome various environmental factors. Taking this into consideration, the potential equation can be regarded as:

$$E = E_{RHE} + iR + \eta \quad (2.2)$$

Where iR is an ohmic potential drop of current flow and η is the overpotential. The overpotential can directly reflect the energy efficiency and HER activity of electrolyser, and it is the most important parameter to evaluate the performance of electrodes and electrolysers. When added with electrocatalysts, the overpotential can be significantly reduced. Like shown above, the platinum catalyst

can reduce overpotential to almost zero, and other efficient catalysts can reduce the overpotential to nearly 100mV or less.

The right way to understand water splitting HER process is necessary to gain insight into issues, such as determine the reaction rate and offer directions for the synthesis and improvement of electrocatalysts. The HER rate is highly depend on the pH value of electrolyte for both ACIWE and ALKWE processes. [13] There are two HER mechanisms, Volmer-Heyrovsky and Volmer-Tafel. In an acidic solution, the HER occurs through following steps: [14]

(1) A proton and an electron combined on the catalyst surface which result in an absorption of hydrogen atom:

$$A + H^+ + e^- \rightarrow AH_{ads} \text{ (Volmer reaction)} \quad (2.3)$$

(2) The absorbed hydrogen atom combined with a proton and an electron to form a hydrogen molecule:

$$AH_{ads} + H^+ + e^- \rightarrow H_2 + A \text{ (Heyrovsky reaction)} \quad (2.4)$$

(3) Two absorbed hydrogen atoms combined and produce a hydrogen molecule:

$$AH_{ads} + AH_{ads} = H_2 + 2A \text{ (Tafel reaction)} \quad (2.5)$$

In alkaline solution, the high pH leads to different Volmer-Heyrovsky and Volmer-Tafel mechanisms of HER process: [15]

(1) According to the low concentration of protons, molecular H_2O instead of H^+ combined with an electron which results in an absorbed hydrogen atom on the catalyst:

$$H_2O + e^- + A \rightarrow AH_{ads} + OH^- \text{ (Volmer reaction)} \quad (2.6)$$

(2) The hydrogen atom combines with a molecule H_2O and an electron to form a hydrogen molecule:

$$AH_{ads} + H_2O + e^- \rightarrow H_2 + OH^- + A \text{ (Heyrovsky reaction)} \quad (2.7)$$

(3) Tafel reaction is the same as ACIWE process. Two absorbed hydrogen atoms are combined to produce a hydrogen molecule:

$$AH_{ads} + AH_{ads} = H_2 + 2A \text{ (Tafel reaction)} \quad (2.8)$$

In the equations, *A* represents the hydrogen absorption site and AHads represents the absorbed hydrogen atom at the site.

The HER process starts with the proton discharge step (equation (4)) and followed with two possible hydrogen desorption pathways, the Heyrovsky reaction (equation (5)) and the Tafel reaction (equation (6)). The HER mechanism can be generalized from Tafel plot derived from polarization curve. [16] An important parameter which can represent the performance of electrocatalyst and reflect the experimental results of Tafel plot is the Tafel slope, and also help explain the HER mechanisms at active sites. For example, in alkaline solutions, for Pt/C electrodes, the HER rate is controlled by Volmer or Volmer-Heyrovsky step and have the Tafel slope range around 120 $mVdec^{-1}$. However in acidic solutions, if the rate-limit step is controlled by Volmer reaction, then Tafel slope is around 120 $mVdec^{-1}$. Otherwise, if the rate-limit step is controlled by Heyrovsky and Tafel reaction, then the Tafel slope should be at the range of 30~40 $mVdec^{-1}$. [17] However, the value of Tafel slope can be affected by many other factors such as applied potential or mass transport in porous structure.

2.2 ELECTROCATALYSTS OF HER

2.2.1 Noble Metal Based Electrocatalysts

PGMs such as Pt, Ru, Rh, Ir and Pd, have been proved as excellent cathode catalysts for hydrogen evolution reaction. Among them, Pt is the most efficient and stable HER electrocatalyst in acidic and alkaline electrolytes. Because of its high cost, there are three major improving methods to better utilize it reasonably and efficiently: (1) increase the number of reactive sites by fabrication of the Pt surface with a nanostructure for arrangement of atoms on the surface to expose more [1 1 0] Pt surface; (2) deposit monolayer Pt on low-cost materials as the alternative to PGM electrocatalyst; (3) make PGM-Metal alloy to increase the active site activity.

Designing a micro- or nano- structure catalyst is an efficient way to increase the surface area. As water electrolysis always occurs on surface of catalysts, a nanostructured catalyst not only has more active sites per unit geometry area, but also facilitates the diffusion of ions, electrolyte and generated gas. Previous studies have already designed and fabricated PGM-based nanostructured catalyst with well-controlled shape and geometry. Synthesis of PGM catalysts with porous nanostructures is another useful method to increase the surface area and activity of electrocatalysts. Previous studies chose dealloying, template synthesis and surfactant-assistant synthesis to prepare porous PGM electrocatalysts for improving activity. However, those porous PGM catalysts may dissolve in various experimental environments and show their poor long-term stability in different solutions.

Many previous researches have shown that [1 1 0] surface of Pt has a higher activity than other surface like [1 0 0] and [1 1 1], and thus the hydrogen adsorption on inner layer have a trend as Pt(111) > Pt(100) > Pt(110). [18]As a result, it is necessary to control the structure of Pt. According to recent researches, Pt nanocrystals with a controlled shape and morphology have been synthesized through various chemical routes in different solvent system. Those Pt nanomaterials with controlled shape can greatly increase the catalytic activity.

In order to reduce the loading amount of Pt, researchers have been finding low-cost materials to replace or reduce parts of Pt amount and make Pt-like catalysts. Previous research shows that transition metal carbides like Mo_2C and WC can be the ideal support to deposit platinum. Data show that Pt/Mo_2C and Pt/WC provide triple and double enhanced HER activity compared with traditional Pt/C catalyst. Besides, Nb_4C_3 and Cr_3C_2 were also proved to be excellent materials to replace carbon. Density Functional Theory (DFT) results show that WC and Mo_2C have similar electronic properties as Pt, in this case they can support Pt to make better catalysts. Recently, researchers have already developed Pt-based noble metal catalysts like Pt-WC, Pt-Mo_2C and Pt-W_2C and they all showed comparable activity and stability as Pt catalyst. Conclusively, modification of Pt on low cost materials can not only reduce noble metal content but also enhance the HER activity. Additionally, morphology and microstructure also affect the activity and catalytic properties of materials.

2.2.2 Non-Noble Metals and Composites

In past researches, people make efforts to find suitable materials for replacing PGMs, and amount large investigate on non-noble metals, results show that those metals have poor activity and stability. Data shows the measurement of 31 non-noble metals using cyclic voltammertic methods, and found the catalytic activity order of non-noble metals is Ni > Mo > Co > W > Fe > Cu. [19]

Normally, metallic cathodes are not suitable for HER reaction. But with the development of cathodes nanostructured surface and the assistant of conductive carbon nanotubes (CNT), this objective can be easily achieved. For example, Ni-CNT and N-graphite have already been studied and show high chemical activity and low onset overpotential. However, these materials have a limitation of unstable performance in alkaline electrolytes because hydride species are formed on the catalyst surface. To improve the performance of non-noble metals, people use TM alloys and compositing metals with some other supports and catalysts to change the electronic structure and increase the surface area.

2.2.2.1 Metal-Free Alloy

Nickel-based alloys or other compositions are the most popular cathode materials because of their low cost and competitive activity with PGMs, they also show high resistance in alkaline solution. Previous researches have studied Ni-based alloy for long time, and many people devote Ni alloy to TMs. Several binary

Ni-based alloys on mild-steel substrates for HER process have been studied and results showed that the catalytic activity order of different alloys is NiMo > NiZn > NiCo > NiW > NiFe > NiCr. NiMo catalyst shows the best activity and stability. In this case, binary or ternary Ni-Mo alloys are considered as the most suitable catalyst for water electrolysis. Their high activity, good stability and low resistance can be explained through hypohyper-d-electronic interactive effect, which can described as Mo in the left half of transition series has empty or half-filled d-electron orbital, and Ni in the other half of transition series with internally paired d-electrons. As a result, by virtue of consummate cooperation in the electrocatalytic reaction, noble-metal like properties can be revealed.

Fe-based alloys are also popular materials for water splitting due to their high hardness, good corrosion resistance and high activity. Researchers have prepared and studied several Fe-R alloys like $Fe_{90}Ce_{10}$, $Fe_{90}Sm_{10}$, $Fe_{90}Y_{10}$ and $Fe_{90}MM_{10}$ (MM: mischmetal which is an alloy of rare earth elements) for the HER in 1M NaOH solution [20]. Results showed that $Fe_{90}MM_{10}$ have the highest activity. This is ascribed to a synergetic effect between the intermetallic phases as a consequence of the change of electronic properties due to the appropriate combination of the 3d 6-orbitals of Fe with the 5d 1-orbitals of La.

Besides alloys in the above, other metals exhibited promising results. For example, Cu-Ti bimetallic electrocatalyst doubles the activity of Pt/C catalyst. The Cu and Ti atoms were considered to create Cu-Cu-Ti hollow sites that have Pt-like hydrogen binding energy.

2.2.2.2 Metal-Free Composites

Although various metals and alloys have been developed for HER, their electrocatalytic activities are still limited by a high overpotential because of an inefficient water decomposition step in alkaline solutions. Also, most of these materials suffer from acid erosion. To overcome these problems, there are two possible ways: (1) adding a second functional component, usually an oxide or hydroxide; (2) enhancing the acidic stability by designing a core-shell structure which have a special shell like graphene to wrap the metal/alloy core.

For the first method, a successful example is the $Ni(OH)_2$ nanoclusters on 9 TM substrates (Cu,Au,Ag,Ir,Ru,Pt,Ni,V,Ti). [21] Results showed that the overpotential of $Ni(OH)_2$/TM for the HER have been greatly reduced compared with pure TM elements. Also, it showed similar activity trends in alkaline solution as in acid solution, Indicating the enhancement of $Ni(OH)_2$ catalyst.

To extend the application of non-noble metals and alloys to acidic solutions, many people use carbon material shell to protect metallic electrocatalysts. For example, a Ni-Sn@C core/shell structure was synthesized by combining the sol-gel, chemical vapor deposition and etching process. [22] This core/shell catalyst had a high conductivity and large active surface area also with good electrocatalyst activity for HER. However, this material is still not suitable for acid solution although it was better than single Fe-Sn. Later, people use CNT as the shell material to protect Fe catalyst and found that CNT not only protect the active metal nanoparticle from

oxidation but also let the desired reactant traverse it. As a result, the Fe/CNT composite showed a high activity in HER even comparable with Pt catalyst. Moreover, long-term test in acidic water electrolysis showed that the CNT shell can largely prevent acid corrosion. [23]

2.2.3 Transition Metal Carbides

Transition Metal Carbides (TMCs) such as tungsten carbides (WC/W_2C) and Molybdenum Carbides (Mo_xC_y), are known to have Pt-like electronic and catalytic properties. People have studied various applications for these materials and their various compositions. Among them, WC and Mo_2C are considered to be more active than other materials. By studying 9 kinds of TMCs, the results showed that Mo_2C have the highest electroactivity, followed by WC and then V_8C_7.[24]

As reported, tungsten carbide is an excellent electrocatalyst for HER with high efficiency and stability. However, during the preparation of tungsten carbide, particle sintering will occur due to the uncontrollable high-temperature carbonization process, this will usually limits the surface area of catalyst. Two popular methods to increase surface area are synthesize porous microstructure and use conductive 3D substrate. Carbon contained gases like CH_4, C_2H_6, CO can be used as the reductive agent of tungsten carbide precursor. Many results showed that the microstructure of material was highly dependent on species of carbon source and the synthesis condition.

2.3 MOLYBDENUM CARBIDE SYNTHESIS AND DEVELOPING STATE

2.3.1 Molybdenum Carbide Catalytic Theory

Metal carbide crystalline structure is based on both geometry and electron factors. Geometry factor can be described by Interstitial compound regulation: When the atomic ratio of nonmetal and metal is lower than 0.59, simple crystal structure is formed. An interesting thing is, although metal carbide has a simple crystal structure, their parent metal always have different crystal structure. For example, metal molybdenum has an bcc crystal structure, but molybdenum carbide has hcp structure, and its carbide-oxide compound has fcc structure. Another factor is electron factor, which based on the bonding action of s-p orbit from non-metal atoms and s-p-d orbit from metal atoms.

From Engel-Brewer theories of metal, the crystal structure of metal or its alloy is depends on the s-p electron number. When the s-p electron number increases, the crystal structure will change from bcc to hcp and then fcc. The metal Molybdenum has bcc structure, Tc and Ru(elements follow Mo) have hcp structure and finally Rh,Pd have fcc structure. This regulation is also observed in Mo, Mo_2C and Mo_2N. This shows that Engel-Brewer theory is applicable for metal interstitial compound. Other metal elements in group IVB~VIB should have the same regulation.

Transition metal carbide compounds have their electron properties based on two factors: (1)The direction and amount of electron transfer, (2)The effect of carbide formation on d- band of metal. Studies shown that the direction of electron transfer in

metal carbide is from metal to non-metal. Electron transfer number is based on the metal element which increased from group IVB to VIB. Carbides formation increase the d- band properties of Mo, makes is similar to group VIIIB, which is noble-metal. Carbon atoms filled into the gap of metal atoms and make the metal-metal distance increase and crystal lattice expands. As a consequence even with fewer electrons, the band is filled to a greater extent. With a normal shape for the d-band the density of states at the Fermi level will be high as it is for the Group VIIIB metals. That is the main reason why transition metal carbide have noble-metal like catalytic properties.

2.3.2 Molybdenum Carbide Structure And Chemical Properties

Molybdenum carbide is a general name for multi-phases of Mo_xC_y, which is formed by Carbon atoms fill into the crystal lattice of metal molybdenum. Based on the ratio of carbon atoms filled, several stochiometries of molybdenum carbides (MoC, Mo_2C and Mo_3C_2) have been reported. Among these different compounds, Mo_2C is considered as the best material with good mechanical properties and chemical catalytic activity. Mo_2C has very high melting temperature at 2770K, also with good hardness and chemical strength. On the other hand, Mo_2C exhibits good chemical activity as an electrocatalyst and high stability at high temperature and. It is considered to be one of the best candidates to replace platinum.

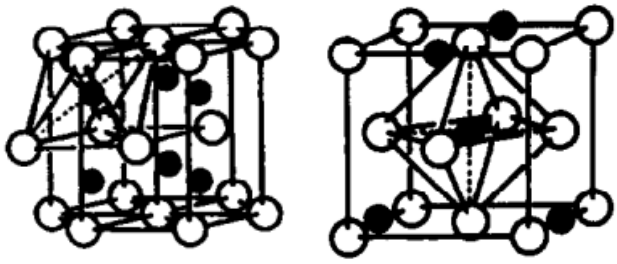

Figure 1 (a)Hexagonal phase(β-Mo_2C) (b) Orthorhimbic face-centered(α-Mo_2C)

Mo_2C has two main crystals structures, orthorhombic phase face-centered (α-Mo_2C) and hexagonal phase (β-Mo_2C). [25] Two phases are stable at different temperature ranges. At low temperature (normally below 1000℃), α-Mo_2C is formed and at high temperature β-Mo_2C is produced. In FCC structure, molybdenum atoms have an ABCABC close-packing structure, and carbon atoms occupy octahedral interstices. In HCP structure, Mo atoms have an ABAB close-packing structure and carbon atoms fill octahedral interstices.

2.3.3 History of Molybdenum Carbide Synthesis

At the very beginning, molybdenum carbide particles was synthesized by directly carbonizing metal molybdenum at over 1000℃, or high-temperature grinding. These synthesis methods were suitable for industrial production, but also had numerous disadvantages like large particle size and difficulty in controlling particle morphology. So in order to prepare high quality Mo_2C catalytic particles,

more methods were developed, like temperature reduction method, sol-gel method, pyrogenic decomposition precursor method, solid phase method and supersonic synthesis method.

For example, Leonard et. al [26,27], synthesized four phases of Mo-C (α-MoC_{1-x}, β-Mo_2C, η-Mo_2C and γ-Mo_2C), by using an amine-metal oxide hybrid method. Measurement of their electrocatalytic activity and stability showed that β-Mo_2C had the best activity, followed by γ-Mo_2C, while other 2 phases had low activity. Bulk Mo_xO_y can be directly used as a cathode in acid or basic electrolysis but shows a lower activity than Pt catalyst. However, increasing the surface area to enlarge the active sites is considered as an efficient way to improve the performance of Mo-C materials. Recent studies have synthesized nanostructured Mo-C through various different organic or inorganic processes, and different morphologies of nanostructured Mo-C have been obtained like nanorods, nanotubes, nanowires and nanospheres. Chen et al. [28] prepared β-Mo_2C nanoparticles by in situ carbulization of ammonium molybate on carbon nanotubes and XC-72R carbon black. The CNT-supported and carbon black-supported molybdenum carbide showed excellent electrocatalyst activity and stability towards HER compared to Mo_2C bulk. Tang et. al. [29] synthesized Mo-C nanowires with 1-D morphology by using a MoO_x/amine hybrid precursor. This nanowire was then used as cathode catalyst for HER. The results showed a very low onset overpotential and a high current density which was higher than commercial and bulk Mo_2C. Later, Tian et. al [30] used p-phenylenediamine as a carbon source and synthesized nanowire and nanosheet

Mo_2C by controlling the ratio of MoO_x and p-phenylenediamine. Wu et. al [31] prepared Mo_2C nanoparticles by using glucose as carbon source and showed an enhanced performance when comparing with bulk Mo_2C.

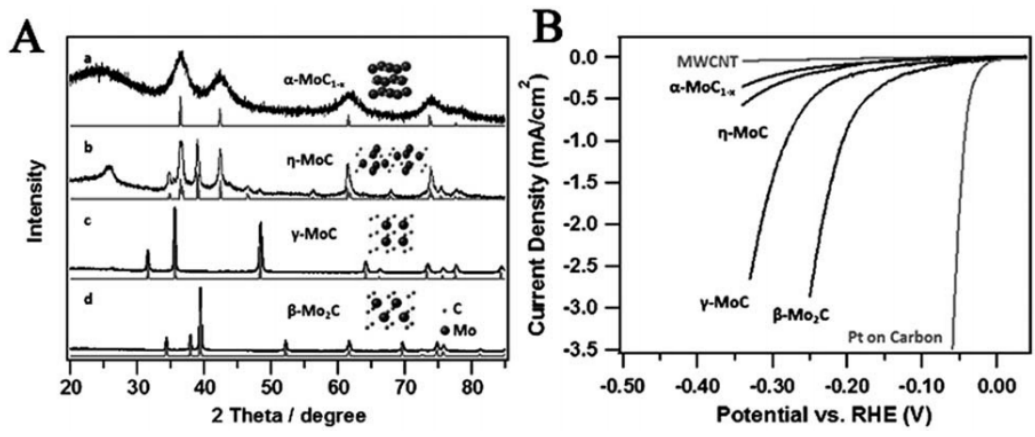

Figure 2 (A)XRD patterns of α-MoC_{1-x}, β-Mo_2C, η-Mo_2C and γ-Mo_2C; (B)Polarization curves of 4 molybdenum carbide and Pt/C, CNTs in 0.1M $HClO_4$. [26]

Besides, the assistance of conductive 3D substrate is an ideal way to increase the surface area, which can also reduce the resistance and facilitate electrolyte and generated gas diffusion. Lee et al. [32] deposited several molybdenum compounds including Mo_2C, MoN and MoS_2, on a carbon nanotube-graphene hybrid support through a modified urea-glass route. Among these catalysts, the Mo_2C/CNT-GO showed the best performance of HER with an overpotential of 62mV and Tafel slope of 58 $mVdec^{-1}$. CNT-GO was reported to reduce aggregation of Mo_2C particles and assist electron transfer.

An excellent Mo_2C base catalyst was prepared by Wang et. al. [33] They modified Mo_xC particles using N-doped carbon vesicles encapsulating Ni nanoparticles using a solid-state thermolysis method. Catalyst composites possess an efficient hydrogen absorption capacity of Ni and a high chemical activity of Mo_xC, thereby, exhibit excellent catalytic performance during HER (almost zero onset potential).

Based on reported researches, it is possible to dope metal elements into lattice of β-Mo_2C. It has been reported that Ni and Fe can been doped into Mo_2C, resulting in the enhancement of electrocatalyst activity for HER. [34,35]

2.4 COMPARING DIFFERENT METHODS OF MoC NANOPARTICLES PREPARATION

Previous studies have shown various methods of Molybdenum Carbide preparation, also different process can effect the mophology of nanostructure. Up till now, some nanostructure Mo-C like nanorods, nanotubes, nanowire, nanospheres, nanosheets have been successfully obtained by researchers. Generally, Mo-C preparation can be divided into four major approaches based on the molybdenum and carbon source and the synthesis process: (1) temperature Programmed Reduction method(TPR); (2) gas phase method; (3) thermal decomposition method; (4) liquid phase method.

2.4.1 Temperature Programmed Reduction Method (TPR)

TPR is a method which reacts metal oxide with gas (hydrogen or nitrogen) through a temperature programmed reduction process. During the process, the ramping rate is controlled to be constant and metal oxide is reducing as the amount of hydrogen gas decreasing. By controlling the current speed of gas, it is easy to calculate the reduction speed by measure the amount of hydrogen gas decreased. It is assumed that only one kind of reduction reaction happened:

$$MO(s) + H_2(g) + CH_4(g) \rightarrow MC_x(s) + H_2O(g)$$

People use GC to test the mixture gas through sample and get the density changing curve of hydrogen gas. This curve is called TPR curve, by analyzing this curve, people can study the Gibbs free energy of metal oxide reduction reaction, interaction of metal and template, interaction of metal and metal oxide, etc.

Boudart et al. [36] developed TPR method in preparing high specific surface area molybdenum carbide. They use molybdenum oxide (MoO_3) and mixture gas (CH_4/H_2), use TPR method to synthesis β-Mo_2C with specific surface area of 50~90cm2/g. They consider that the crystal structure didn't change during the reduction reaction, which means that the carbon atoms replace the oxygen atoms in the crystal and meanwhile the Mo atoms didn't change directions.

In the TPR method, the reactant ratio, current speed of mixture gas, ramping rate are controlled to synthesis products with different components, specific surface area and crystal structure. It is the most widely used method in metal carbide synthesis.

2.4.2 Gas Phase Method

This method always use high specific surface area activated carbon (higher than 200cm2/g) and high volatility transition metal compounds mixed in a certain ratio and react under 900~1400 ℃ for a long period of time, then cool the products in nitrogen gas and get the final powder. Y. J. Zhang et al. [37] reported that they use high specific surface area activated carbon and MoO_3 powder to synthesis β-Mo_2C at 1300℃ in argon atmosphere. Their ratio of C:Mo is 6:1, and specific surface area of Mo_2C is 213cm^2/g.

The disadvantage of gas phase method is the high temperature required and the uncontrollable of reaction condition. In addition, this method has low efficiency in product synthesis, so its not widely used.

2.4.3 Thermal Decomposition Method

Thermal decomposition method is the organic reaction of metal oxide or metal halide with certain organic compound. The reaction first forms a metal-organic compound and then thermal decomposed in nitrogen or argon atmosphere. This method has a high transfer efficiency so its suitable for large scare manufacture. The following sol-gel method is also a thermal decomposition method.

2.4.4 Liquid Phase Method

Low temperature liquid phase method is the reaction by dissolving all reactants in certain solvent and use a mild condition to synthesis materials. Manish Patcl et al. dissolved four-water ammonium molybdate and disaccharide(C12H22O11) in water to form the solution and leave it in air for 5~6 days until dry, then use 70~80℃ and 230℃ in vacuum to fully dry the water and collect the black powder. They anneal the black powder in 1200℃ and get Mo_2C powder. The particle size of Mo_2C is 3nm.

Liquid phase method has a comparably milder reaction condition and can synthesis Mo_2C with high specific surface area.

However, in recent studies, people are using mixture methods to synthesis Mo_2C, its hard to divide them into the above four methods.

Giordano et al. [38] have suggested a sol–gel-like synthetic route. While conventional methods employ crystalline species, the sol–gel like fabrication approach uses a polymeric metal precursor as the starting material. In this fabrication tactic, urea and ethanol are utilized as a carbon source and ratio of urea/metal precursor determines the phase of the final product.

In this study, a facile synthesis route of Mo_2C nanoparticles via microwave-assisted solvothermal reaction has been investigated. In addition, we have demonstrated that Mo_2C nanoparticles are synthesized at one-step from polymeric metal precursors under microwave irradiation. This is different from previous studies that have coated crystalline solid carbon with Mo2C nanoparticles to synthesize a

highly conductive composite material. Microwave induces localized heat and creates a ‘hotspot’ that develops a highly crystalline structure in final products. Due to the molecular level interaction of the microwave with the reagent species, reaction time and temperature are also reduced. In this work, we examine the performance of Mo_2C nanoparticles as the counter electrode of the electrochemical cells.

3.0 RESEARCH DESCRIPTION

3.1 HYPOTHESIS

The first hypothesis of this study is that the crystal structure and morphology of molybdenum carbide can be controlled by changing a ratio of urea/Mo in a precursor solution. This is due to a change in the chemical activity of carbon in the precursor. The second hypothesis of this study is that the MWSV method can produce particles that require lower temperature annealing to form Mo_2C due to a volumetric heating effect.

3.2 OBJECTIVES

The objective of this study is to examine the effect of reactant ratio and annealing temperature on the crystal structure and electrochemical properties of to Mo_2C particles that are produced from MWSV method. By comparing microwave-assisted solvothermal method and previously reported sol-gel method, study on the role of the microwave heating is also planned.

3.3 RESEARCH TASKS

The first task of this thesis is preparing Mo_2C nanoparticles by using MWSV method in different Mo:C ratio and anneal at different temperature, by measuring XRD and SEM data to show the changing of crystallinity and crystal structure, and whether MWSV can provide a lower synthesis temperature. The second task is to coat Mo_2C nanoparticle films on substrates, characterize a catalytic performance of Mo_2C nanoparticle film during electrolysis, and compare the results with other previously reported results. This is expected to show the effect of temperature and ratio.

4.0 EXPERIMENTAL SECTION

4.1 PREPARATION OF Mo_2C THROUGH MWSV METHOD

Molybdenum(V) carbide ($MoCl_5$ 99.6%, Alfa Astar), ethanol (200 proof, Decon) , and urea (Sigma Aldrich) were used to synthesize Mo_2C nanoparticles. In a typical process, 2 g of pure ethanol was mixed with 1 g of $MoCl_5$ and a different amount of urea was added into the mixture. The precursor solution was stirred for 2 min and loaded in a teflon vessel. The sealed teflon vessel was irradiated with microwave (Mars, CEM) for 10 min. During the reaction, the temperature was controlled to be 150 ℃. A pressure sensor was used to monitor any change in pressure inside the vessel. After the microwave reaction, solid nanoparticles were collected using a centrifuge and annealed at 600, 700, 800 and 870℃ for 3 hrs.

Microwave reaction process program:

Ramping rate: 5.7℃/min;

Maximum protection temperature: 150℃;

Maximum protection pressure: 800ksi;

Holding time: 10min;

Maximum power: 800W.

Annealing process program:

Ramping rate 3.3℃/min;

Ramping time: 180min(600℃ maximum), 210min(700℃ maximum), 240min(800℃ maximum), 260min(870℃ maximum);

Holding time: 180min;

Cooling rate: 3.3℃/min;

Protection gas: Nitrogen (99.9%),

Protection gas current speed: 1ml/s.

4.2 CHARACTERIZATION

After synthesis, the nanoparticles were analyzed with a suite of characterization tools. The crystal structure of Mo_2C nanoparticles grown by the MWSV method was examined by X-ray diffraction (XRD) method (Philips, PW-1810 diffractometer, Cu-K radiation, λ= 1.54 Å). The scan range is 20~80(degree), the scan time is 12min. The morphological trait of the nanoparticles was characterized by field emission-scanning electron microscope (FE-SEM, Philips XL-30).

4.3 Mo_2C FILMS PREPARATION

Mo2C films were prepared by screen printing of Mo_2C nanoparticle paste onto FTO substrate. The NSG ETCTM FTO substrate was chosen as the substrate of Mo2C with a resistivity of 8 Ω/sq. FTO glass was first cut into 2cm×2cm size substrate and washed by acetone and ID water for 20min in each solvent.

Mo_2C nanoparticle paste was composed of Mo_2C nanoparticles, ethanol, α-terpineol and ethyl cellulous. The Mo_2C nanoparticles was first fully separated in mixture of ethanol and DI water solvent by repeatedly stirring and ultrasonic dispersion for 10min each step and repeated for 5-10 times. Then, a certain amount of cellulous was dissolved in ethanol. As the cellulous dissolve very slow, we slightly heated the solution up to 50 ℃ and make it dissolve quickly. Afterward, use centrifuge to separate the above Mo_2C nanoparticles solution and get the thin nanoparticle with black thick parts added to cellulous solution. Adding α-terpineol and keep stirring the whole system with slightly heating to 50 ℃ for 30min. Then repeatedly use strong ultrasonic to fully mix those components and make the solution stable and uniform until the solution become thick enough. Last step is using 3-roll grinding to homogeneously grind and distribute the Mo_2C nanoparticles. The Mo_2C paste was coated on FTO glass through a screen printing process, and organic parts in the paste were burned at 220~250 ℃. Higher burning temperature will reduce the burning time and the remained organic parts. The electric conductivity was tested through a four point probe method.

4.4 MEASUREMENT OF HER PROPERTIES FOR Mo_2C MATERIALS

The electrocatalyst activity and electrochemical performance for HER was tested by a cyclic voltammetry (CV) measurement technique. A CV work station needs three electrodes: reference electrode, working electrode and counter electrode.

This is also called a three-electrode setup. In the measurement, we use Saturated Calomel Electrode(SCE) as the reference electrode and Pt electrode as the working electrode. While our sample Mo_2C electrode is the counter electrode. Three different pH states of electrolytes were used during the test including 0.5M H_2SO_4, 0.5M Phosphate buffer and 1M NaOH.

The measurement can be divided into liner sweep voltammetry (LSV) test and current-resistance (I-R) test. LSV test measure the overpotential of Mo_2C electrodes and I-R test for long-term stability. Normally, people use the overpotential at the current density of $10mAcm^{-2}$ to reflect the activity of elctrocatalyst activity for HER. During the measurement, we set the potential range from -1.0V to +1.0V in order to cover the $10mAcm^{-2}$ current density point. For IR stability test, we set the potential at 0.5V to see the stability of each electrode, and remaining time is 30min. However, Mo_2C electrode may dissolve rapidly in alkaline state electrolyte so we could no longer use 1M NaOH as the electrolyte.

The polarization curve can be obtained by using LSV data. After measurement of the above electrochemical tests, we draw the Tafel plot of Mo_2C electrodes and calculate the Tafel slope. By comparing overpotential and Tafel slope with previous studies, we can know how much enhancement this material has compared with the traditional Pt and Mo_2C bulk.

5.0 EXPERIMENTAL RESULTS AND DISCUSSION

In this section, SEM, XRD, HER data are shown to explain the effect of temperature and ratio condition. All different conditions are shown in the following table for easy comparison.

Table 2 Mo_2C data content

T(℃) / R	600	700	800	870
5	XRD HER		XRD SEM HER	XRD SEM
6	XRD HER		XRD HER	
7	XRD HER	XRD	XRD SEM HER	XRD SEM
8	XRD HER		XRD HER	
9	XRD HER		XRD SEM HER	XRD SEM

(R=urea/Mo mol ratio)

5.1 PARTICLE STRUCTURE OF Mo_2C NANOPARTICLE

Figure 3 shows morphology of Mo_2C particles which were synthesized using different R ratio (R=5,7,9). The particles were annealed in an inert ambience at T=870℃.

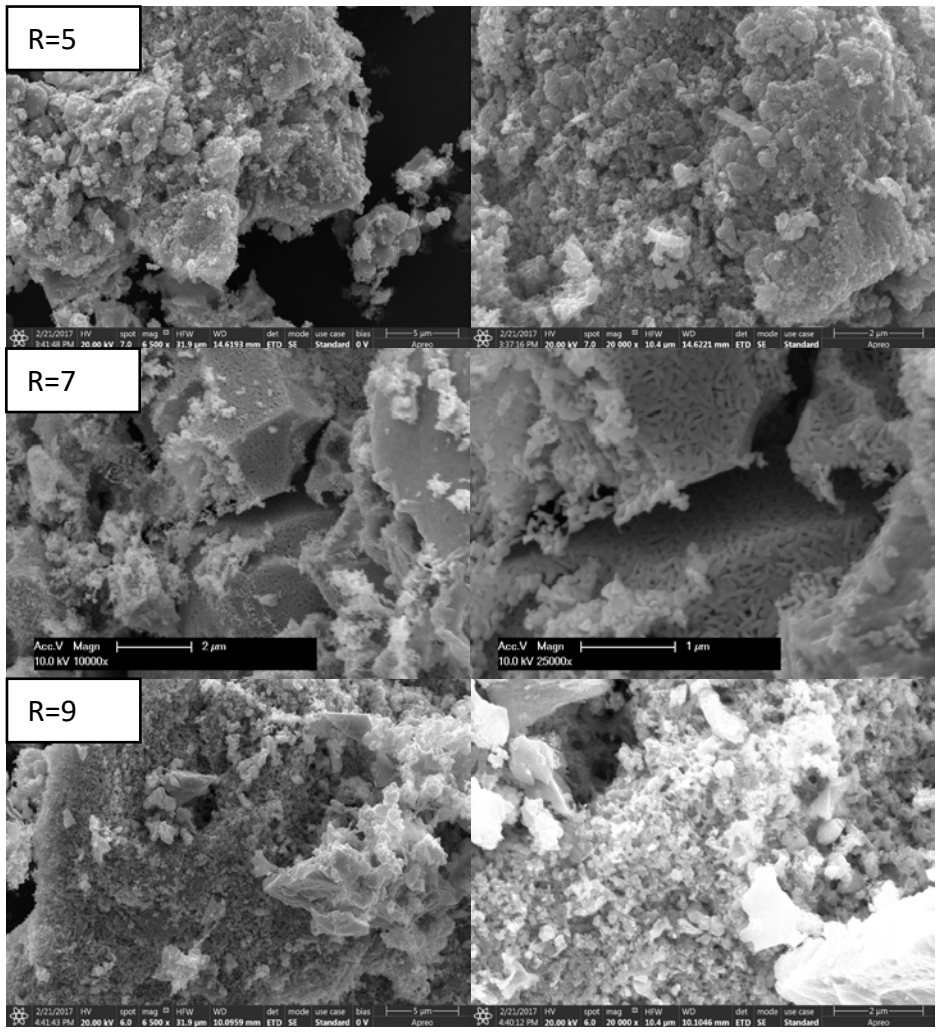

Figure 3 SEM of Mo_2C (T=870℃ R=5,7,9)

SEM images show 2 different structures. One is polyhedral structure and the other is cotton-shaped structure. A polyhedral structure is composed of Mo_2C particle and a cotton-like structure is composed of MoO_xC_y and Mo_xC_y. An increase in R ratio of the precursor solution increases a relative volume of the cotton-shaped region. This indicates that an increase in the carbon content promotes the incorporation of carbon atoms into a Mo lattice and forms non-stoichiometric molybdenum carbide.

5.2 CRYSTALLINE PHASE OF Mo2C NANOPARTICLES

A change in the crystal structure of molybdenum carbide particles during thermal annealing was studied by XRD measurements. XRD patterns of thermally annealed particles are shown in Figures 4 (a)~(d). Figures 4 (a)~(c) presents the crystal structure of particles which were prepared from different R ratio and annealed at same temperature (600, 800, 870 ^oC). Figure 4 (d) shows the crystal structure of particles (R=7) as a function of annealing temperature.

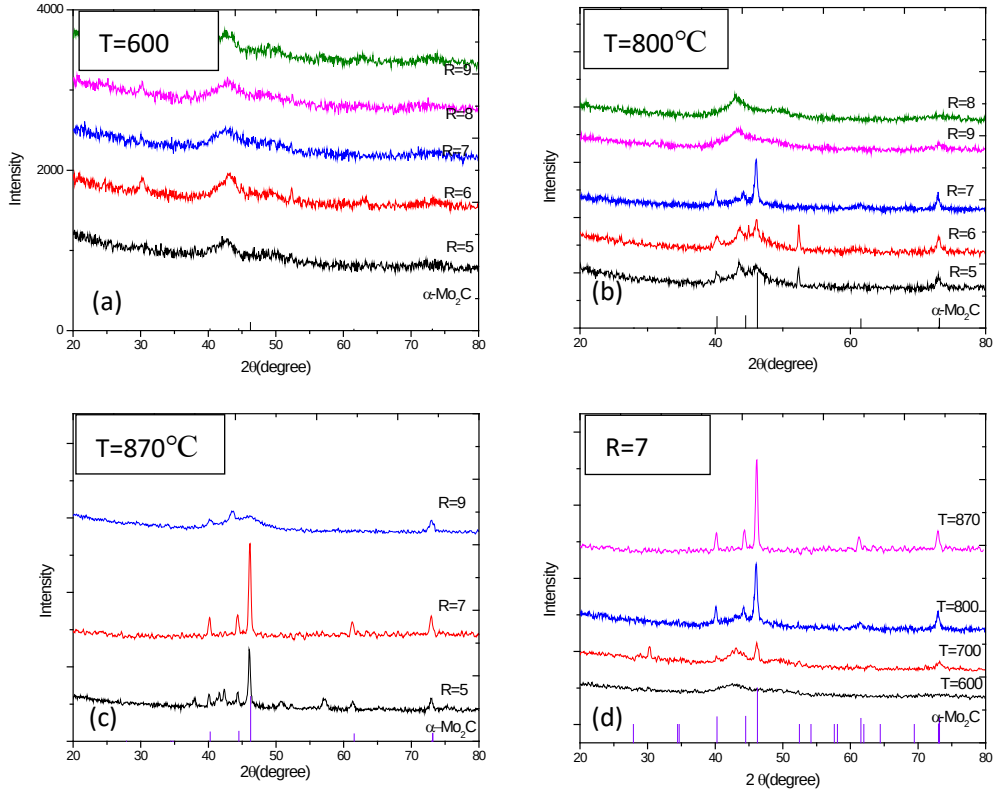

Figure 4 XRD of Mo_2C with different R at (a) 600℃ annealing; (b) 800℃ annealing; (c) 870℃ annealing; and same R at different temperature(d) R=7.

When comparing samples at certain temperature with different ratio condition, it is obviously shown on Figure 4 (b) that crystallinity is increasing follow the order of ratio increasing that R=5 < R=6 < R=7. However, if R continues increasing, the stoichiometry of particles change and the crystal structure becomes different from Mo_2C. As seen from the XRD pattern in Figure 4 (a), particles annealed at 600℃ do not show sharp peaks. This means that the crystallinity of particles is very low and

the precursor is not fully converted to molybdenum carbide. As annealing temperature increases, the crystalline structure of α-Mo_2C is improved. It is noted that the highest crystallinity is obtained when R ratio of the precursor is 7 (see Figures 4 (b), (c)). A comparison of particles (R=7) which were annealed at different temperature indicates that the amorphous phase disappears between 800 ^oC and 870 ^oC (see Figure 4 (d)). When R is smaller than 7, the crystallization is retarded and a mixture of molybdenum carbide and molybdenum nitride appeared at $T \geq 800\ ^oC$. This indicates that nitrogen in urea can participate in the chemical reaction if a chemical activity of carbon decreases. Particles derived from precursors of R=8 and 9 shows a very broad peak in XRD patterns even after 870 ^oC annealing. This is attributed to addition of more carbon atoms into Mo FCC lattice. Additionally added carbon atoms suppress the crystallization and precursors remain amorphous.

5.3 HER PERFORMANCE OF Mo_2C ELECTRODES

Crystal structure and microstructure shown in previous sections show that highly crystalline α-Mo_2C particles with high surface area can be synthesized by MWSV and subsequent annealing at 870^oC. In this study, HER activity of Mo_2C particles is measured using a potentiostat that has three electrodes: reference electrode, working electrode and counter electrode. This is also called a three-electrode setup.

In the measurement, we use Mo_2C particle film as a counter electrode. Saturated calomel electrode (SCE) is a reference electrode and Pt wire is a working electrode.

5.3.1 Stability of Electrodes in Different pH

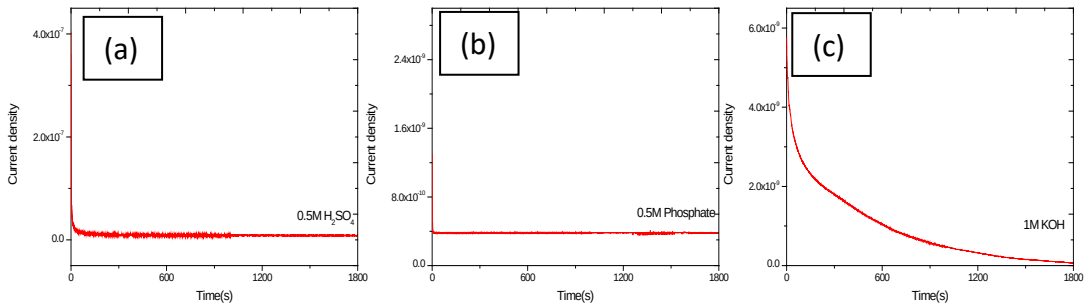

Figure 5 I-t curve of Mo2C in different electrolyte (a)0.5M H2SO4, pH=0.3; (b)0.5M phosphate, pH=7.0; (c)1M KOH, pH=13.9

Figure 5 shows a long-time stability of Mo_2C electrode film in different pH electrolytes. For this end, I-t measurement was done for 30 minutes. When bias is applied to electrodes in an acidic solution, output current flowing between counter electrode and working electrode does not change over time. In neutral electrolyte, current density is stable in the beginning. However, Mo_2C film starts dissolving in 20 minutes and current density also starts decreasing. In a basic electrolyte condition, Mo_2C film is dissolved from the beginning, which means that KOH solution is not

suitable for CV test of Mo_2C electrode. In a following electrochemical characterization (LSV test), 0.5M H_2SO_4 is chosen so that Mo_2C particle film does not degrade during an electrolysis process.

5.3.2 Measurement of Overpotential of Molybdenum Carbide Electrode

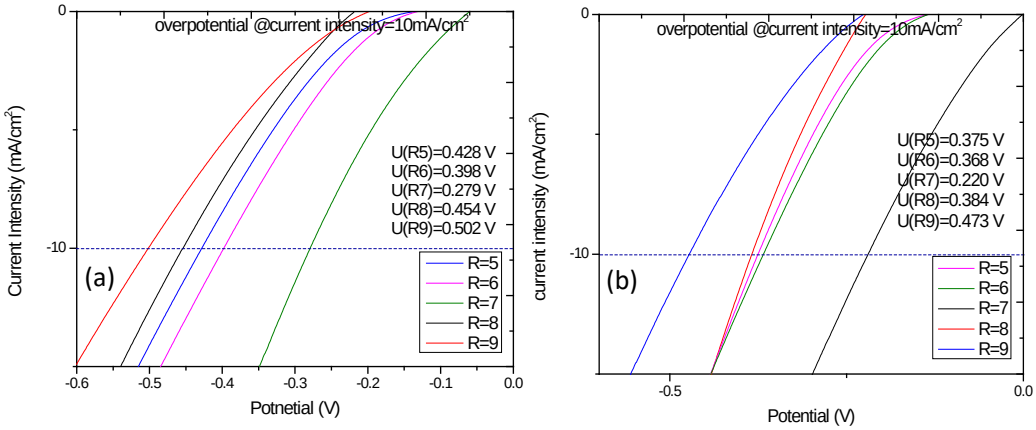

Figure 6 LSV curve for different ratio condition at (a) T=600°C (b) T=800°C in electrolyte 0.5M H_2SO_4

The overpotential of the electrolysis has a direct impact on the energy efficiency of the electrolyser, and it is a very important parameter to evaluate the performance of electrodes and electrolytes.

In previous studies, electric potential producing current density of 10mA/cm^2 during HER is designated as the overpotential of the electrode. The lower the overpotential, the higher the HER activity of the electrode. Figure 6 shows the

overpotential of Mo_2C electrodes which are prepared using different R and annealing temperature. Results show that the overpotential of molybdenum carbide electrodes is very sensitive to a carbon content of the precursor. Mo_2C particles from the condition R=7 exhibit the best electrocatalyst activity, which is consistent with XRD analysis results showing the highly crystalline α-Mo_2C without any second phase. When R decreases from 7 to 6, the overpotential of 800 ^oC annealed films increases from 220 mV to 360 mV. An increase in the overpotential of molybdenum carbide from conditions of R = 5, 6 is attributed to the appearance of molybdenum nitride. When R increases to 9, the overpotential of molybdenum film increases to 470 mV. This is due to a dramatic decrease in the crystallinity of Mo_2C which is confirmed in XRD analysis.

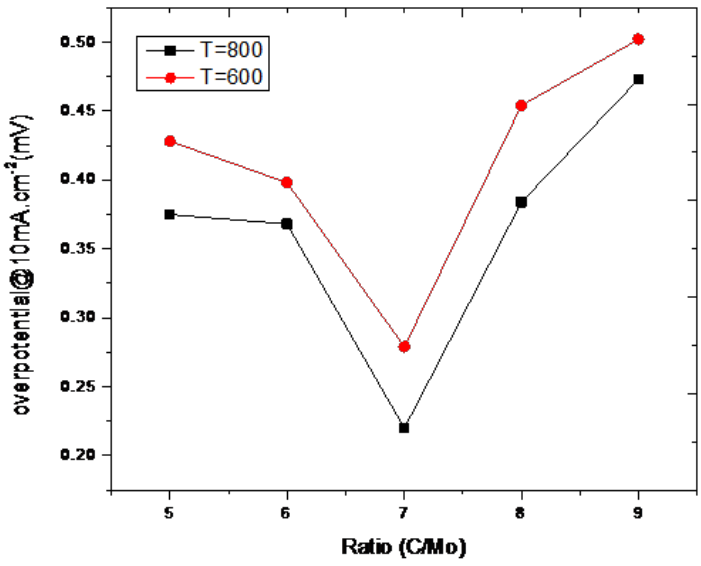

Figure 7 overpotential vs. Ratio condition

A similar dependence of the overpotential on R is observed in films which are annealed in T=600℃ and 800.(from figure 7) This suggests that the chemical activity of carbon during MWSV is a critical parameter which determines the HER activity of molybdenum carbide films.

5.3.3 Comparison of Tafel Slope

In LSV measurement, the results of overpotential measurement can be largely influenced by details of experimental setup (e.g. material type and shape of working electrode, electric current, pH and ion concentration of electrolyte). To exclude the effect of unknown variables in evaluating the performance of molybdenum carbide electrodes, a slope of Tafel plots is widely used as another performance indicator of electrode material. Tafel plot comes from Tafel equation on a change in the overpotential as a function of current density. In Tafel plot, a slope A represents the electrochemical kinetics by connecting the rate of electrochemical reaction to the overpotential. For one single electrode, the equation is:

$$\eta = \mathrm{A} \times \ln(\frac{i}{i_0}) \tag{5.1}$$

Where η is the overpotential, A is the so-called ‘tafel slope’, i is the current density and i_0 is the ‘exchange current density’.

The exchange current density shows the rate at which oxidized and reduced species in an electrolyte transfer electrons with electrodes at equilibrium without external bias. This exchange current shows the rate of reaction in a reversible

potential (i.e. in an equilibrium condition) and indicates how well materials perform as a catalysts. Exchange current (i_0) of Pt is 0.794 mA/cm^2 which is several orders of magnitude larger than that of most metals. In addition, a slope of Tafel plot (A) is inversely proportional to the charge transfer coefficient on the surface of electrode during HER. The charge transfer coefficient shows the portion of the interfacial electric field participating redox reactions (i.e. reducing the barrier height of HER rection). Therefore, smaller Tafel slope in HER means that electrode materials convert electric energy to chemical energy more effectively.

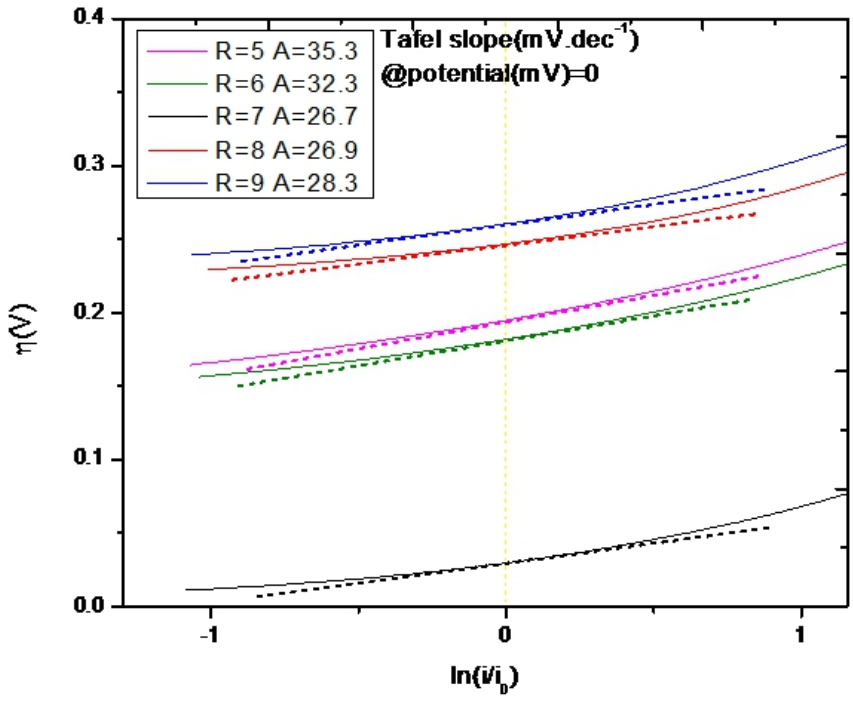

Figure 8 Tafel plot of Mo_2C of different ratio condition at T=800℃

Figure 8 shows Tafel plot of molybdenum carbide electrodes annealed at T=800 ^{o}C during HER. Analysis results show that the electrode synthesized at the condition of R=7 exhibits the lowest slope, 26.7 mV/dec. Tafel slopes confirm that Mo_2C films in this study is a good catalyst for HER. The best values from our study are compared with results of recent reports. The performance of the electrode from this study is comparable to or better than that of pure Mo_2C electrodes and even Mo_2C/graphene electrodes.

Table 3 HER results from references

catalysts	overpotential η(mV)	Tafel slope ($mV.dec^{-1}$)	reference
α-Mo2C NPs	220	26.7	this thesis
Mo2C/CNT	152	65	Energy Environ. Sci. 2013,6,943
Mo2C microparticles	225	55	Angew. Chem. Int. Ed. 2012,51,12703
MoC-Mo2C-6.81	218	52	Chem. Sci., 2016, 7, 3399
MoC	221	101	Chem.Sci., 2016, 7, 3399
Mo2C-carbon nanocomposite	260	--	J.Mater.Chem.A., 2014, 2, 10548
Mo2C nanoparticles decorated graphitic sheet	210	--	ACS Catal, 2014, 4, 2658

5.4 DISCUSSION

Discussion in this section demonstrates the effect of urea/Mo ratio, annealing temperature on the reaction path, morphology, crystal structure, and electocatalytic activity of Mo_2C particles. Compared with sol-gel method, MWSV method has several distinctions in a reaction path to molybdenum carbide. Detailed differences are summarized below.

Both sol-gel and MWSV methods use $MoCl_5$, ethanol, and urea as starting chemicals. The first step of a chemical reaction is to mix $MoCl_5$ and ethanol. In this step, molybdenum-orthoester is formed as a transition state and color of solution turns to dark green:

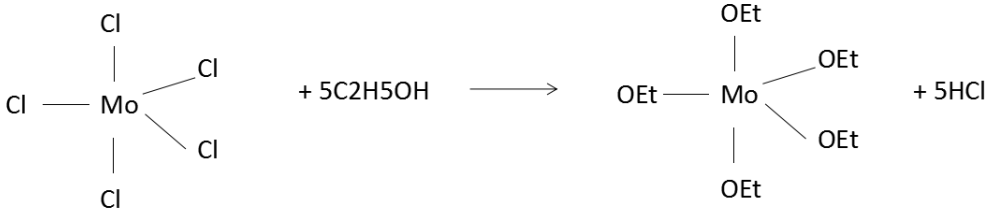

This transition chemical is not stable and can easily react with ethanol:

$$Mo(EtO)_5 + EtOH \rightarrow Mo(EtO)_4OH + Et_2O \quad (5.2)$$

Et_2O is ether, which will quickly evaporate from the solution at room temperature. $Mo(EtO)_4OH$ is a partially hydrolyzed molecule. Two hydrolyzed molecule can link together in a condensation reaction, such as:

$$Mo(EtO)_4OH + Mo(EtO)_4OH \rightarrow (EtO)_4Mo\text{-}O\text{-}Mo(EtO)_4 + H2O \quad (5.3)$$

$$\text{or} \quad Mo(EtO)_4OH + Mo(EtO)_4OEt \rightarrow (EtO)_4Mo\text{-}O\text{-}Mo(EtO)_4 + EtOH \quad (5.4)$$

This condensation reaction can polymerize molybdenum-orthoester molecules and build larger molecules. Possible structure of molybdenum-orthoester molecules can be a chain, a ring, or a mixture of chain and ring.

Chain reaction:

$$n\left(HO\text{-}Mo(EtO)_3\text{-}OH\right) \rightarrow HO\text{-}\left(Mo(EtO)_3O\right)_n\text{-}H + nH2O \tag{5.5}$$

Ring reaction:

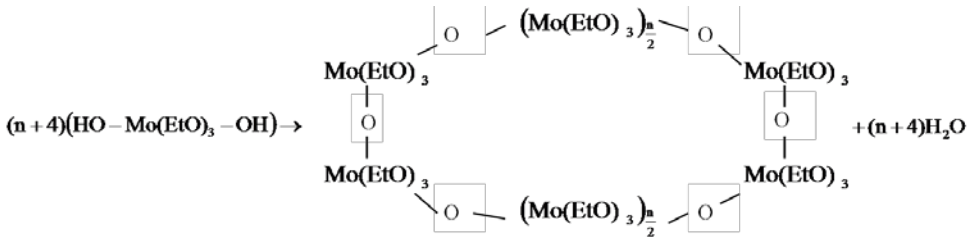

(5.6)

When molybdenum-orthoester is mixed with urea, intermediate Mo products containing nitrogen are precipitated. In sol-gel method, this precipitate is converted to molybdenum carbide through solid-state transfer process by high temperature annealing.

Microwave assisted process provide high pressure and high energy radiation, which make the polymer molecule have decomposition reaction to form Mo-O-C-N glassy compounds while some of the nitrogen products are decomposed into NH_3 or NH_4Cl and easily separated from solid precipitates. Subsequent thermal annealing process converts solid precipitates to molybdenum carbide and enhances the crystallinity of particles. Mo-C-N-O glassy precipitate is first transformed into MoOxCy or MoNx at low temperature annealing. This is due to the diffusion of carbon and nitrogen. At high temperature, glassy MoO_xC_y and MoN_x are crystallized into Mo_2C or MoC_x. In previously studies, α-Mo_2C was preferably obtained in

850~900 ^{o}C and β-Mo_2C was found at 1000~1400 ^{o}C. Thermal annealing temperature also influences the morphology of Mo_2C nanoparticle. SEM images (Figure 9) shows the microstructure of Mo_2C particles which were annealed at 800 ^{o}C and 870 ^{o}C.In higher magnification images, spherical particles were found at T=800℃ and rod type particles was observed at T=870℃.

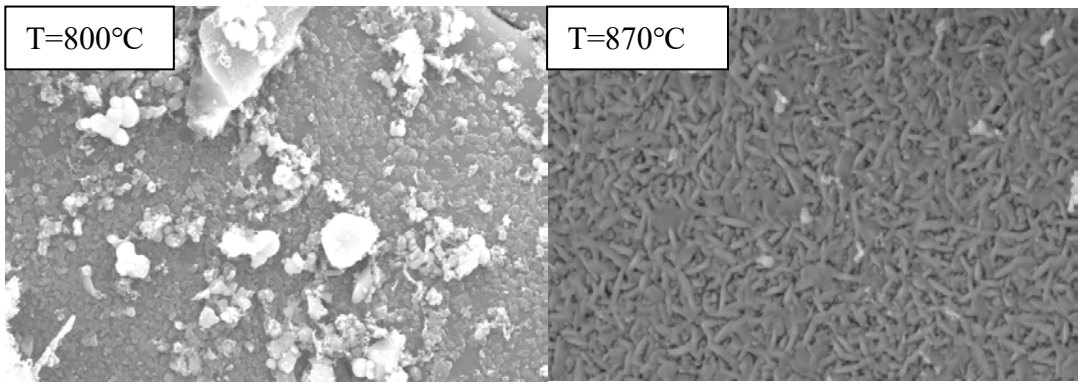

Figure 9 SEM with magnification 25000x of Mo2C (R=7 T=800℃ and 870℃)

In crystal structure analysis, it is noted that α-Mo_2C and β-Mo_2C have very similar structures and peak locations in their XRD patterns are almost identical. Only a small difference between α-Mo_2C and β-Mo_2C is a ratio of peak heights. A relative intensity of (1 0 0) at 2θ = 40.25 ^{o}, (1 0 1) at 2θ =46.25 ^{o}, and (1 1 0) at 2θ =73.15 ^{o} is 20.8, 100 and 17.7 in α-Mo_2C. In β-Mo_2C, a relative intensity of (1 0 0) at 2θ = 40.16 ^{o}, (1 0 1) at 2θ =46.17 ^{o}, and (1 1 0) at 2θ =73.15 ^{o} is 18.0, 100 and 16.1. From XRD patterns of Mo_2C samples, XRD peaks at 2θ=40.25 and 46.25 always have an

intensity ratio of 1:5. This shows that molybdenum carbide particles synthesized by MWSV is α-Mo_2C. From synthesis conditions of R=5 and R=9, a very broad peak is observed at 2θ = 40 ~ 50 º under sharp peaks of α-Mo_2C. This is indexed as glassy MoO_xC_y and Mo_xC_y. At the conditions of R=8 and 9, sharp peaks disappear in XRD patterns. Instead, a broad peak is found. Since the carbon activity is high, the lattice is overfilled by carbon atoms and a ratio of Mo:C is 2:(1+x). When extra carbon atoms fills empty space between Mo atoms, the metallic bond is elongated and the unit cell is distorted. If only 2 carbon atoms filled into the FCC Mo crystal structure, the expansion of all direction is almost the same, but when more carbon atoms filled, the expansion is nonuniform and the crystal structure warped into uncertain morphology.

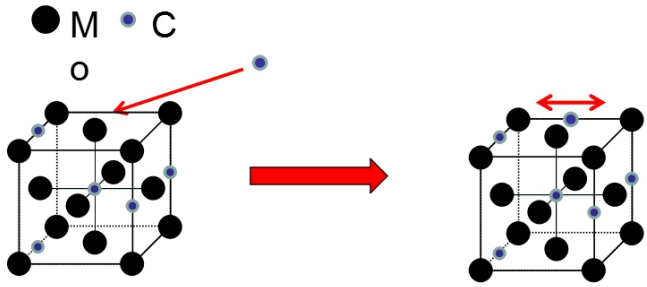

Figure 10 Lattice change when more than 2 carbon atoms filled

When R is too large and much extra carbon atoms are formed, we cannot control the number of extra fill, as a result the Mo_2C transfer into MoC_x. In lower R

conditions, this overfill will become incomplete fill or incomplete replacement. The metal-orthoester polymer have a MoO_2-$(OR)_x$ molecule, the carbon atoms will gradually replace the oxygen atoms in Mo lattice or fill the lattice gap of Mo. In case of insufficient carbon source, the replacement is not complete, part of the oxygen atoms and carbon atoms filled into Mo lattice and form the MoO_xC_y compound, this compound also have uncertain chemical stoichimetric number, as a result the crystal structure and morphology is unstable which shown as cotton-like structures in SEM image.

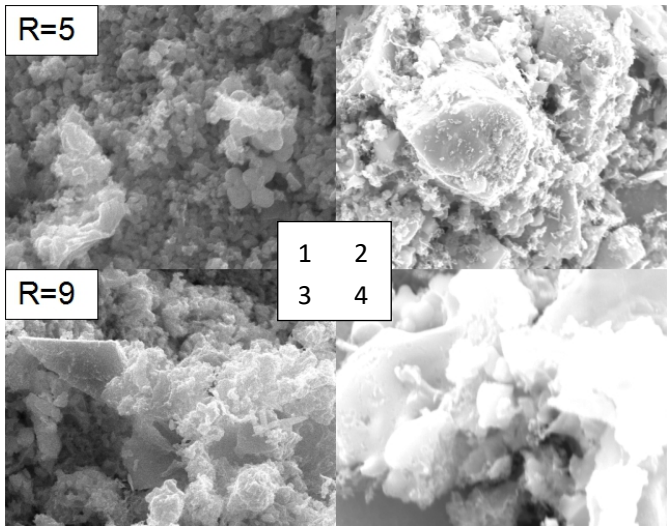

Figure 11 Cotton-like structure SEM of MoO_xC_y and Mo_xCy ((1)R=5 T=800℃; (2)R=5 T=870℃; (3)R=9 T=800℃; (4)R=9 T=870℃.)

As discussed in a previous chapter, HER activity is affected by two main factors. In addition, for a certain electrode material, smaller particle size means larger sepcific surface area which promotes catalytic reactions on the electrode surface. In previous reports, simple α-Mo_2C or Mo_2C mixed with different types of carbon molecule exhibit the overpotential ranging from 130 mV to 260mV. Multi elements doped Mo_2C compounds have the overpotential value of 60~140mV. The best overpotential from MWSV synthesized Mo_2C is 220mV which is comparable to state-of-the art results in literature. The condition of best overpotential is R=7, T=800℃, the HER results shown from R=5 to 9 is a clearly 'V' trend (Figure 7), R=7 is the lowest point of the curve at both T=600 and 800 conditions.

For a large range LSV test (-1.0~1.0), the electrode activity is continuously changing. People always use data in -0.5~0 range to calculate the tafel slope, as the curve always doesn't follow a strictly Log curve, the slope is very different at high potential range. Take the case of sample R=7, T=800℃ in this thesis, the tafel slope is 26.7 at η=0V, 66.9 at η=1V and 124 at η=2V, this change is due to the curve itself. Ideal tafel curve have a $y = e^x$ shape at lower potential and $y = ax + b$ shape at higher potential. For a more fairly comparison, the tafel slope data of η=0V is used to compare with previously results because in those references, tafel slope value is at η=0V. In future LSV test, data around η=0V is easily affected by environment, so the data at higher potential range will be more convincing.

6.0 CONCLUSION

This study examines two important physical and chemical properties of Mo_2C particles grown by MWSV method, crystal structure and electrocatalytic activity during HER, as a function of a reactants ratio and annealing temperature. For this purpose, a series of Mo_2C samples in same ratio and different temperature condition and also same temperature but different ratio condition was synthesized. By comparing data collected through XRD, SEM and LSV, we get the following conclusions:

(1) A reactant ratio, R=7 condition can produce Mo_2C of high crystallinity and excellent HER activity, in comparison to the ratio of R=5, 6, 8, and 9. In R=5 and 6 conditions, the low carbon source will cause by-product MoO_xC_y formation while the lower ratio, the lower percentage of Mo_2C crystal. In R=8 and 9 cases, extra carbon atoms fill interstitials of Mo lattice and distort the crystal structure, leading to the glassy MoC_x phase. The difference of product component in low ratio conditions and high ratio conditions also show the priority of carbon atoms fill into the lattice interstitial.

(2) Higher annealing temperature produce Mo_2C with better crystalline structure and better HER activity, but the Mo_2C cannot be synthesized at temperature lower than 700℃. The annealing process is the reaction of decomposition and atom replacement. For temperature lower than 700℃, the energy isn’t enough for carbon to

replace oxygen completely. As a result, large amount of MoO_x and MoO_xC_y is formed. When temperature is high enough, the replacement will not restricted by energy so Mo_2C is formed. The higher annealing temperature, the replace reaction is faster and the crystalline structure will be better.

BIBLIOGRAPHY

[1] H. Ibrahim, A. Ilinca and J. Preeon, *Renewable Sustainable Energy Rev.*, 2008, 12, 1221-1250.

[2] Z. Ying, X. Zheng, G. Cui, *Energy Converse. Manage.*, 2016, 115, 26-31.

[3] S. Hu, L. Xu, L. Wang, D. Li, P. Zhang, S. Chen, Int. *J. Hydrogen Energy*, 2016, 40, 773-783.

[4] S. Ye, R. Wang, M.-Z. Wu, Y.-P. Yuan, *Appl. Surf. Sci.*, 2015, 358, 16-27.

[5] M. Gannouni, I. Ben Assaker and R. Chtourou, *Int. J. Hydrogen Energy*, 2015, 40,7252-7259.

[6] S. Chen, S. S. Thind and A. Chen, *Electrochem. Commun.*, 2016, 63, 10-17.

[7] H. Wu, *Appl. Energy*, 2016, 165, 81-106.

[8] S. Trassati, *J. Electroanal. Chem.*, 1999, 476, 90-91.

[9] M. Carmo, Int. *J. Hydrogen Energy.*, 2013, 38, 4901-4934.

[10] E. Fabbri, *Catal. Sci. Technol.*, 2014, 4, 3800-3821.

[11] F. Safezadeh, E. Ghali and G. Houlachi, *Int. J. Hydrogen Energy*, 2015, 40, 256-274.

[12] M. Bajdich, M. Garicia-Mota, *J. Am. Chem. Soc.*, 2013, 135, 13521-13530.

[13] J. Durst, A. SieBel, C. Simon, *Energy Environ. Sci.*, 2014, 7, 2255.

[14] Y. Li, J. Wang, X. Tian, L. Ma, C.Dai, Z. Zhou, *Nanoscale*, 2016, 8, 1676-1683.

[15] Q. Lu, G.S. Hutchings, *Nat. Commun.*, 2016, 6, 6567.

[16] J. O. M. Bockris, E. C. Potter, *J. Electrochem Soc.*, 1952, 99, 169-186.

[17] G. Eliezer, Physical Electrochemistry, John Wiley, New York, 2011.

[18] N. M. Markovic, B. N. Grgur and P. N. Ross, *J. Phys. Chem. B*, 1997, 101, 5405-5413.

[19] M. Miles and M. Thomason, *J. Electronchem. Soc.*, 1976, 123, 1459-1461.

[20] F. Rosalbino, D. Maccio, E. Angelini, A. Saccone and S. Delfino, *J. Alloys Compd.*, 2005, 403, 275-282.

[21] N. M. Markovic, *Angew. Chem.*, 2012, 124, 12663-12666.

[22] M. Gong, W. Zhou, J. Yang, *Nat. Commun.*, 2014, 5, 4695.

[23] M. Tavakkoli, T. Kallio, O. Reynaud, *Angew. Chem.*, 2015, 127, 4618-4621.

[24] Y. N. Regmi, J. M. Thode and B. M. Leonard, *J. Mater. Chem. A*, 2015, 3, 10085-10091.

[25] S. T. Oyama, Departments of Chemical Engineering and Chemistry, Clarkson University, Potsdam, New York, 13699-5705, USA.

[26] C. Wan, Y. N. Regmi and B. M. Leonard, *Angew. Chem.*, 2014, 126, 6525-6528.

[27] C. Wan, N. A. Knight and B. M. Leonard, *Chem. Commun.*, 2013, 49, 10409-10411.

[28] W.-F. Chen, *Energy Environ. Sci.*, 2013, 6, 943-951.

[29] Q. Gao, C. Zhang, H. Xu, Y. Tang, *Chem. Mater.*, 2009, 21, 5560-5562.

[30] C. Ge, P. Jiang, W. Cui, Z. Pu, Z. Xing, J. Tian, *Electrochem. Acta*, 2014, 134, 182-186.

[31] C. Tang, A.Sun, Y. Xu, Z. Wu, D, Wang, *J. Power Sources*, 2015, 296, 18-22.

[32] D. H. Youn, S. Han, J. S. Lee, *ACS nano.*, 2014, 8, 5164-5173.

[33] S. Wang, J. Wang, M. Zhu, X. Bao, Y. Wang, *J. Am. Chem. Soc.*, 2015, 137, 15753-15759.

[34] K. Xiong, Z, Wei, *J. Mater. Chem. A*, 2015, 3, 1863-1867.

[35] C. Wan and B. M. Leonard, *Chem. Mater.*, 2015, 27, 4281-4288.

[36] M. Boudart, *J. Sol. State Chem.*, 1985, 59, 332-347.

[37] Y. J. Zhang, *Sci. Commun.*, 1997, 42, 488-491.

[38] C. Geordano, *Nano. Letters*, 2008, 12, 4659-4663.